

The Fourpoint Antenna as a LEDA Outrigger Antenna

Steve Ellingson*

Aug 6, 2011

Contents

| | | |
|----------|--|-----------|
| 1 | Introduction | 2 |
| 2 | The EDGES Fourpoint Antenna | 2 |
| 3 | NEC Model for the EDGES Fourpoint Antenna | 2 |
| 4 | A Candidate LEDA Outrigger Antenna | 8 |
| 5 | Considerations for Future Work | 8 |
| 6 | Acknowledgments | 13 |

*Bradley Dept. of Electrical & Computer Engineering, 302 Whittemore Hall, Virginia Polytechnic Institute & State University, Blacksburg VA 24061 USA. E-mail: ellingson@vt.edu

1 Introduction

LEDA (“Large aperture Experiment to detect the Dark Age”) is an augmentation of LWA1, the first station of the Long Wavelength Array. One aspect of LEDA will be the addition of new “outrigger” antennas located far from the station’s primary array of 257 stands. A frequency-scaled version of the “fourpoint” antenna employed by the EDGES (“Experiment to Detect the Global EOR Signature”) project has been proposed for this purpose. In this report, we consider the performance of a scaled version of this antenna as a LEDA outrigger antenna. Section 2 describes the existing EDGES fourpoint antenna. In Section 3, we describe an electromagnetic model for the existing EDGES fourpoint antenna and validate the model by comparison to published data. In Section 4, this model is scaled in frequency to obtain a LEDA-appropriate design, and the effects of realistic ground and a ground screen are considered.

2 The EDGES Fourpoint Antenna

The EDGES fourpoint antenna is shown in Figure 1 (from [1]). It is adapted from a design originally described in [2]. The antenna is essentially two “thick” dipoles arranged to give orthogonal linear polarizations. Each dipole is intended to be a good match to a balanced 50Ω load.

Each dipole consists of two four-sided sheet metal “pedals”. The geometrical definitions used in this report to describe the pedals are shown in Figure 2. Note that the design as shown in Figure 2 is completely described by the parameters b (“side length”), α (length of longest diagonal relative to $\sqrt{2}b$), w (width of the gap between edges of adjacent pedals), and h (height above ground). Apparent in Figure 1 but not included in the geometrical model is a “lip” around the edge of each pedal formed by a upturned section of metal. The lip is significant, and will be taken into account as described later in this report.

A useful description of the EDGES fourpoint antenna is given in Rogers & Bowman (2008) [3]. From Figure 1 of this reference, the “tip-to-tip” length of a dipole ($2c + \sqrt{2}w$ in terms of the variables in use in this report) is 0.8λ at 200 MHz, which is 120.00 cm, and $h = 0.3\lambda$ at 200 MHz, which is 45.00 cm. The side length b and gap width w are taken to be 30.48 cm and 2.40 cm, respectively, from EDGES Memo 69 [4]. These choices imply $c = 50.30$ cm and $\alpha = 1.35$.

A drawing provided separately by Alan Rogers confirms $b = 30.48$ cm, but indicates $2c + \sqrt{2}w = 0.9\lambda$ at 200 MHz, suggesting $\alpha = 1.52$. This drawing also indicates the height of the lip around the circumference of the pedal is 1/2-in (1.27 cm). The lip increases the capacitance between the pedals, resulting in a reactive impedance with roughly the same overall variation as without the lip, but which is centered closer to zero. This has the effect of improving and broadening the match.

3 NEC Model for the EDGES Fourpoint Antenna

NEC-4.1 [5] is used for electromagnetic modeling in this report. Each pedal is represented as a wire grid as shown in Figure 3. The grid uses one segment between junctions, and the minimum segment length is 1.905 cm (0.0127λ at 200 MHz). The wire radius a is 0.2 cm, which satisfies both the “equal area rule” for wire grid modeling of solid sheets and NEC guidelines generally. All wires are assumed to be perfectly conducting. Each dipole’s feed is modeled as a single wire of 3 segments connecting the interior vertices, with the center segment taken to be either the source or a load. The diameter of the feed wire is 0.1 cm, and intersection between feed wires is avoided by separating the dipoles vertically by 0.3 cm (0.002λ at 200 MHz). In the results which follow, the x -oriented dipole is driven with a voltage source while the y -oriented dipole is loaded with a 50Ω resistance. Ground is assumed to be infinite and perfectly conducting.



Figure 1: The EDGES fourpoint antenna (from [1]).

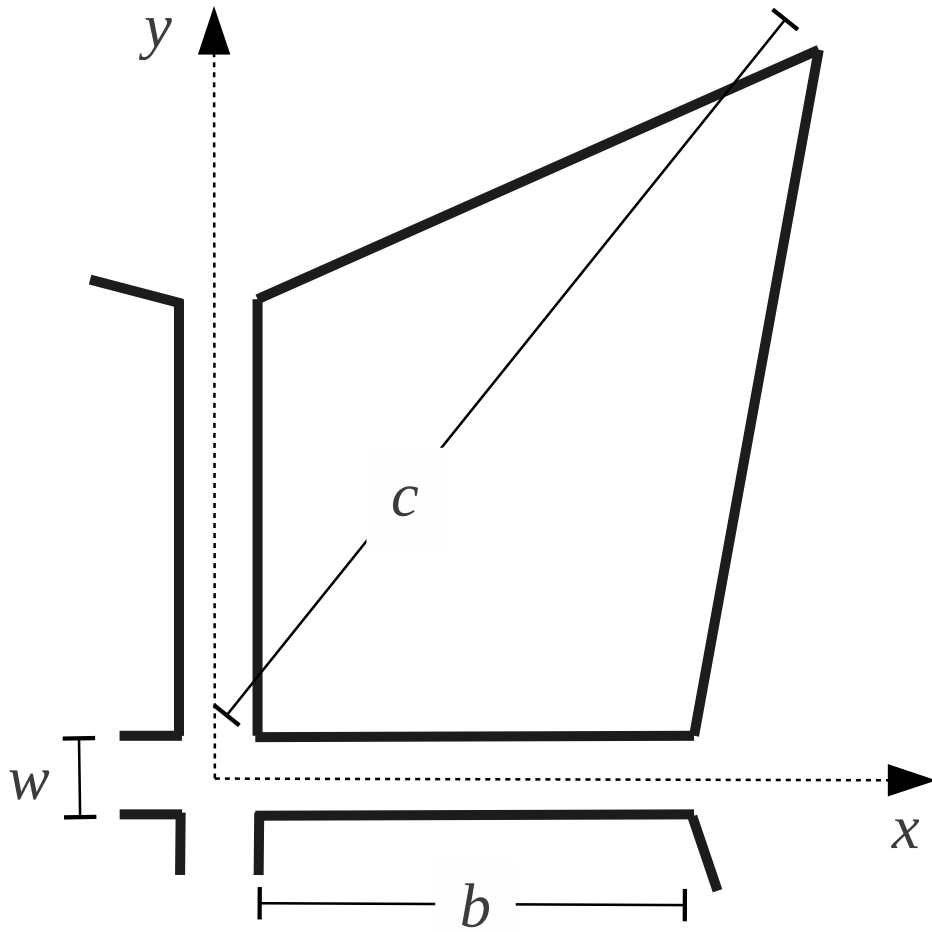


Figure 2: Geometrical definitions used in this report. The relationship between c and b is given by $c = \sqrt{2ba}$. The pedals lie in the plane $z = h$, where $z = 0$ is the ground.

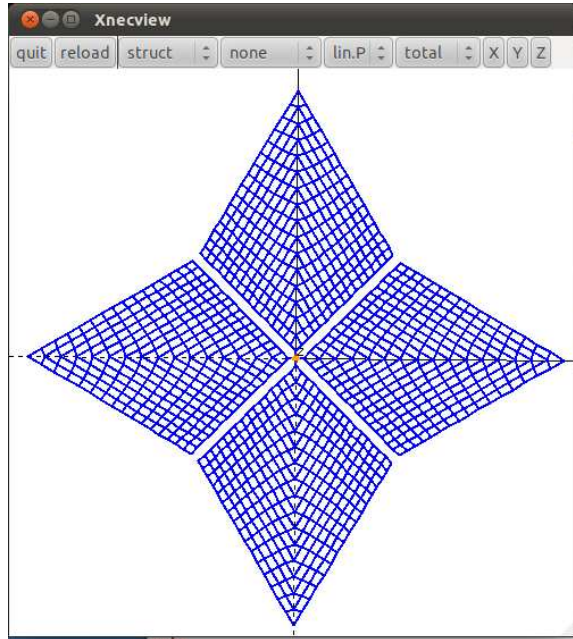


Figure 3: Wire grid used in this report.

As noted above, the actual design includes a 1.27 cm-high lip around the circumference of each pedal. This lip is not explicitly included in this model; however, the relevant effect of the lip is. Since the wires defining the pedal have a radius of 2 mm, the modeled pedals can be interpreted as having an “equivalent thickness” of about 4 mm. However, since the x - and y - oriented dipoles are vertically offset by 3 mm, the “effective” cross-section for estimating capacitance across the pedal-to-pedal gap is only about 1 mm, and probably significantly less because the wire cross-section is circular as opposed to square. Thus, the model can be viewed as having an “equivalent lip height” of somewhat less than 1 mm, relative to the actual lip-height of 1.27 cm. Rather than attempting to explicitly model the lip directly, we can model the increased capacitance by reducing w , noting that the capacitance of an ideal parallel-plate capacitor is proportional to h_l/w , where h_l is (effective) lip height.

Figure 4 shows the magnitude of the reflection coefficient (with respect to 50Ω) for three candidate NEC models, which differ only in α and w . The first (blue/ \circ) uses $\alpha = 1.35$ and ignores the lip issue. The result is significantly worse than the corresponding result shown in Figure 4 of Rogers & Bowman (2008) [3]. Next, w is decreased to 0.6 cm (red/ \times), which should increase the capacitance across the inter-pedal capacitance by a factor of approximately 4. As expected, the result is significantly improved, varying around 0.2 as does Figure 4 of [3]. However, this result suggests an emerging resonance around 200 MHz which does not exist in the Rogers & Bowman result. Increasing α to 1.52 (the other value identified in Section 2) increases the tip-to-tip length and yields a result (green/square) which is reasonably close to Figure 4 of [3].

On this basis, the following set of parameter values is taken to be the best choices for the existing (100-200 MHz) EDGES fourpoint antenna for the purposes of NEC modeling: $b = 30.48$ cm, $\alpha = 1.52$, $w = 0.60$ cm, and $h = 0.45$ cm. The computed self-impedance of this antenna is shown in Figure 5.

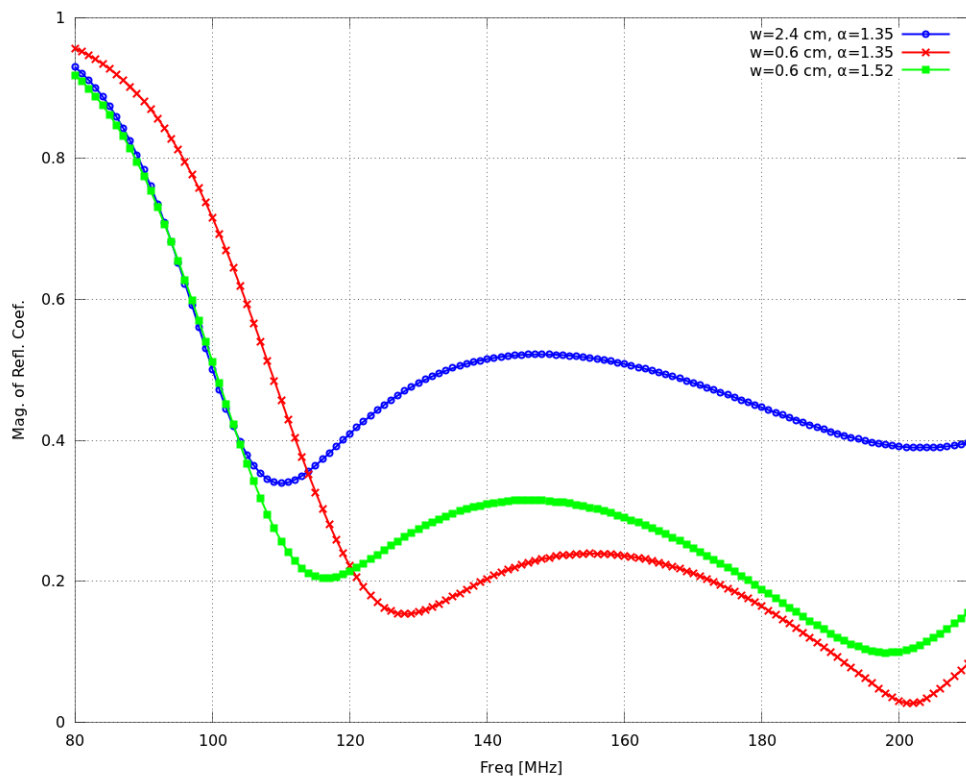


Figure 4: Magnitude of the reflection coefficient with respect to 50Ω for three candidate NEC models of the 100-200 MHz EDGES antenna.

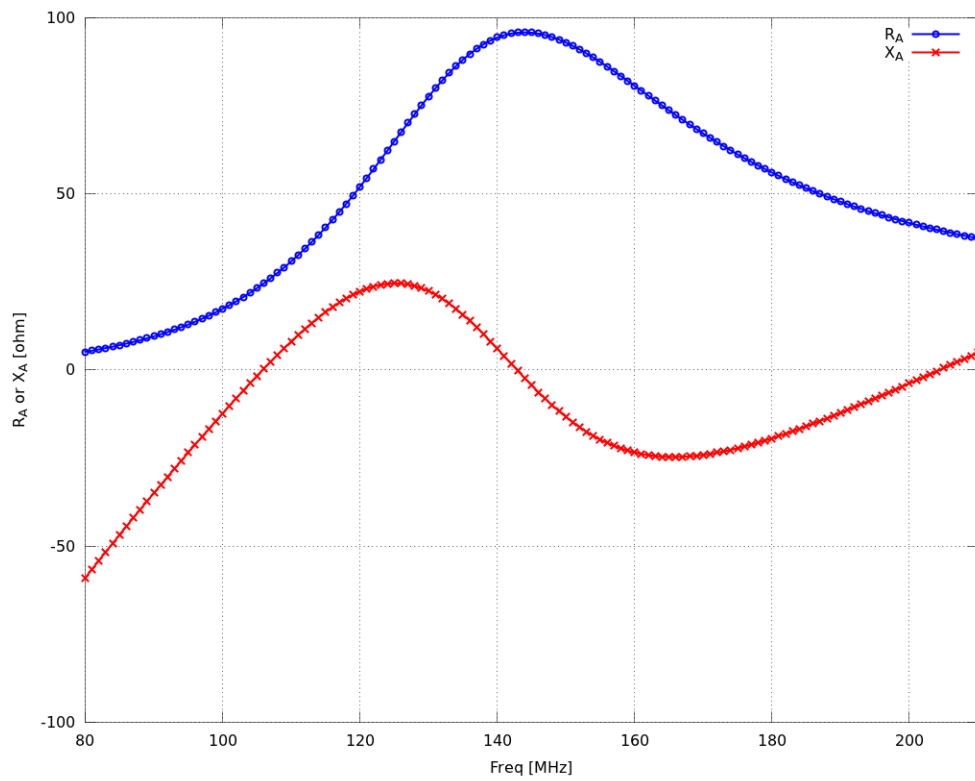


Figure 5: Self-impedance of the selected ($w = 0.60$ cm, $\alpha = 1.52$) NEC model of the 100-200 MHz EDGES antenna.

4 A Candidate LEDA Outrigger Antenna

To obtain a candidate LEDA (30–88 MHz) antenna, the dimensions of the EDGES (100–200 MHz) antenna were simply scaled up by a factor of 3. Thus, $b = 91.44$ cm, $\alpha = 1.52$, $w = 1.80$ cm, and $h = 135.00$ cm. Similarly, all dimensions of the NEC model were scaled by a factor of 3. The resulting reflection coefficient is shown in Figure 6 (curve labeled “PEC”).

Also shown in Figure 6 is the same result computed for ground conditions which are not ideal; corresponding to use of the antenna without a ground screen. The “Very Dry” and “Typical” conditions are representative of the range of possibilities at the LWA1 site, depending on the composition of the soil (which varies spatially) as well as the moisture of the soil (which varies both spatially and temporally). As for LWA1 antennas, the relatively large variation motivates the use of a ground screen.

Rogers & Bowman (2008) [3] describe an octagonal ground screen having maximum diameter 1.3λ at 200 MHz, which is 1.95 m (visible in Figure 1). Scaling up by a factor of 3, the maximum dimension becomes 5.85 m. For simplicity, we here consider a square ground screen 5.8 m on each side, with each side aligned along lines of constant x or y . The grid spacing is set to 10 cm and the wire radius is set to 1 mm, which closely models the ground screen material already in use at LWA1 [6]. The ground screen is located in the $z = 1$ cm plane (as opposed to $z = 0$) to avoid any possibility of NEC-related difficulty in modeling screen-to-ground contact; this also represents the effects of inevitable gaps between the ground screen and the irregular ground surface.

The performance of this ground screen is demonstrated in Figure 7. Note that the inclusion of the ground screen results in performance very close to (but not exactly the same as) the performance achieved in the infinite/perfect ground case. Presumably this result could be further improved by making the ground screen larger and/or making the ground screen wire grid finer.

Co-polarized directivity in the principal planes is shown in Figures 8 and 9 for 30 MHz and 88 MHz, respectively. Again, “typical” (not ideal) ground is assumed and the results with and without the use of the ground screen are shown. Note that the ground screen is a mixed blessing in terms of effect on pattern: Zenith directivity is significantly higher, but horizon gain is in some cases greater (i.e., worse, at least from an RFI perspective). Also apparent in these figures is a high level of “ground loss” – that is, power which is available to the antenna when the ground screen is used, but which is apparently dissipated into the ground otherwise. The ground loss when the ground screen is not used is apparently ~ 3 dB at 30 MHz and somewhat less at 88 MHz, which is consistent with previous simulation and measurement studies at these frequencies [6, 7].

5 Considerations for Future Work

No attempt has been made to optimize the candidate LEDA antenna design presented here. Independently of efforts in that direction, here are a few considerations for future modeling work on this antenna: As noted above, the material used in the antenna and ground screen was assumed to be perfectly conducting; in fact, any material likely to be used in this application (e.g., aluminum) has finite conductivity and will contribute some loss. Also, recall that the inter-pedal capacitance plays an important role in the performance of this antenna, and has been modeled rather crudely here. However, it is straightforward to explicitly model the lip that appears in the original EDGES design and/or the tuning plate proposed in the original work of Suh using the wire-grid approach employed here.

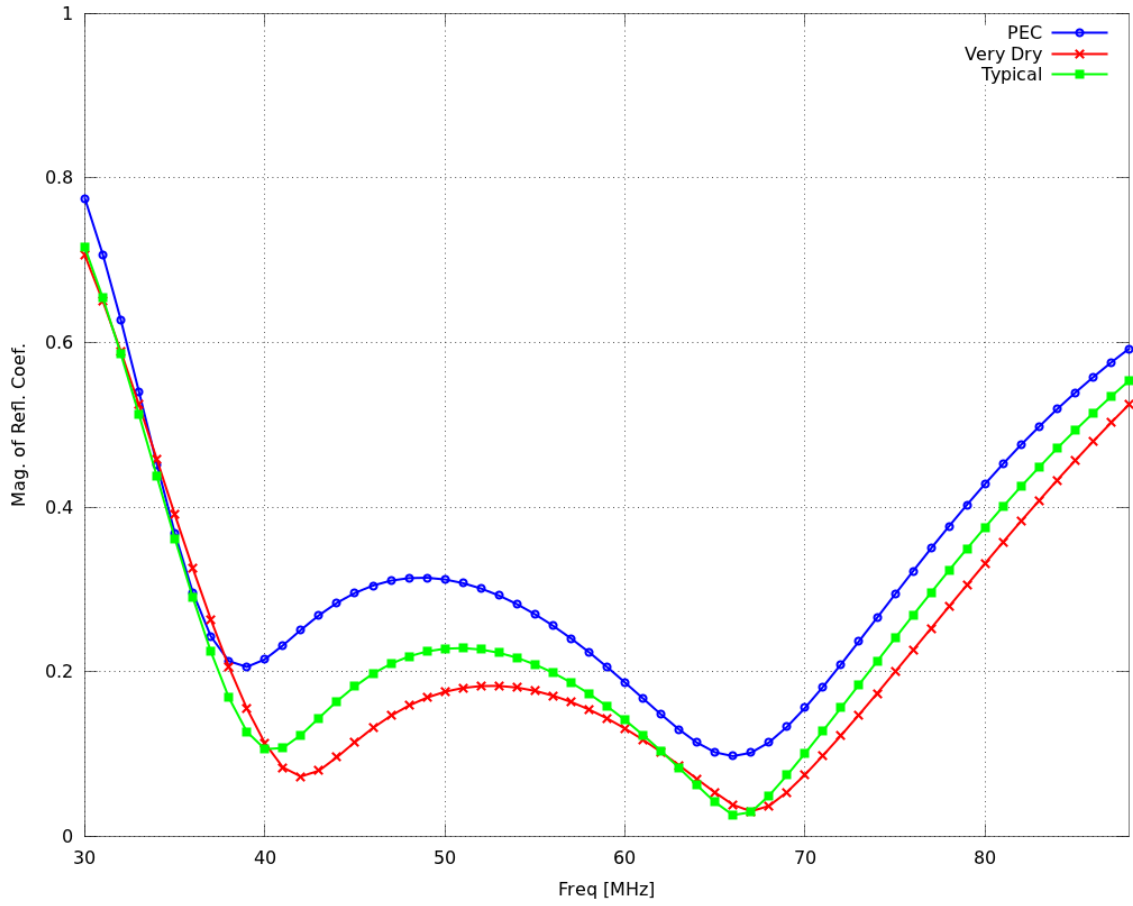


Figure 6: Magnitude of the reflection coefficient with respect to 50Ω for the NEC model of the candidate LEDA antenna, for three ground conditions: “PEC” (perfectly conducting), “Very Dry” ($\epsilon_r = 3$, $\sigma = 100 \mu\text{S/m}$), and “Typical” ($\epsilon_r = 13$, $\sigma = 5 \text{ mS/m}$).

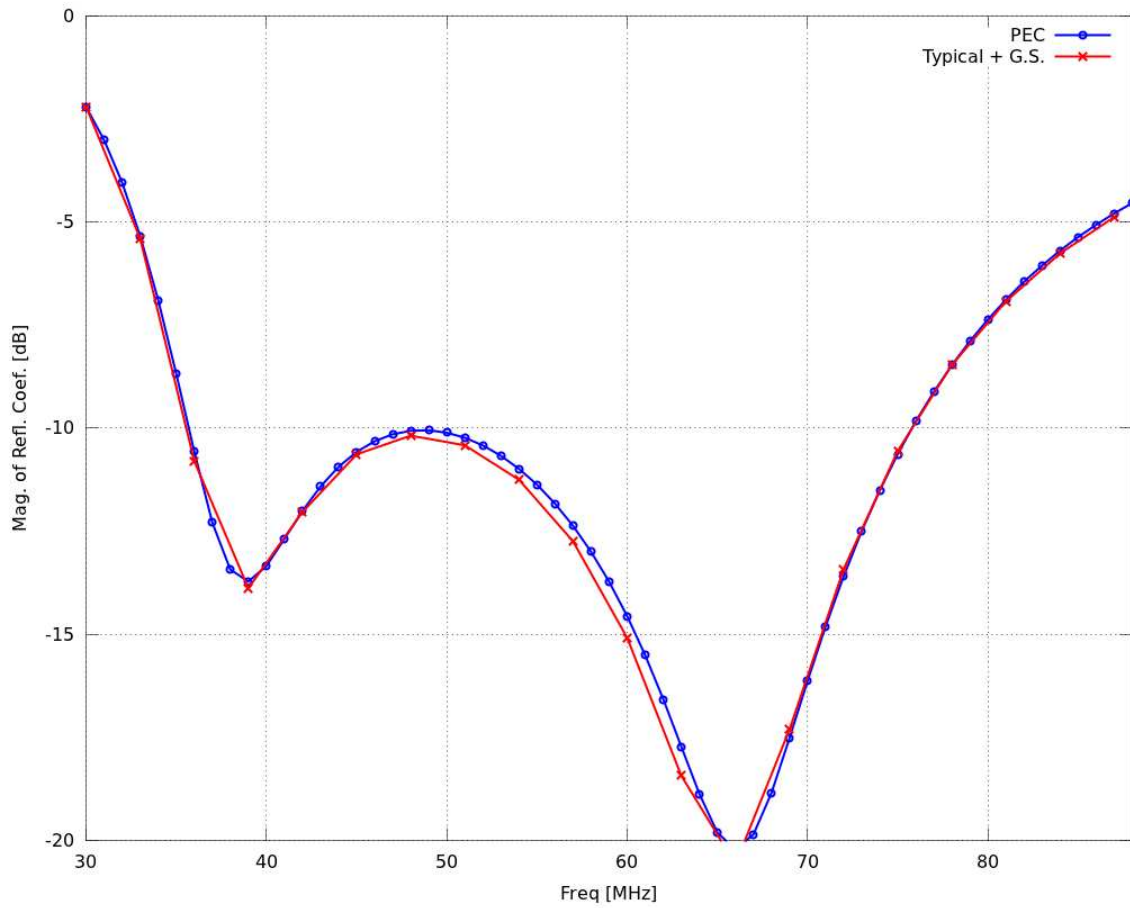


Figure 7: Magnitude (NOTE: now in dB scale) of the reflection coefficient with respect to 50Ω for the NEC model of the candidate LEDA antenna over “typical” ($\epsilon_r = 13$, $\sigma = 5$ mS/m) ground, using the ground screen described in the text. The same result assuming an infinite perfectly conducting ground is shown for comparison.

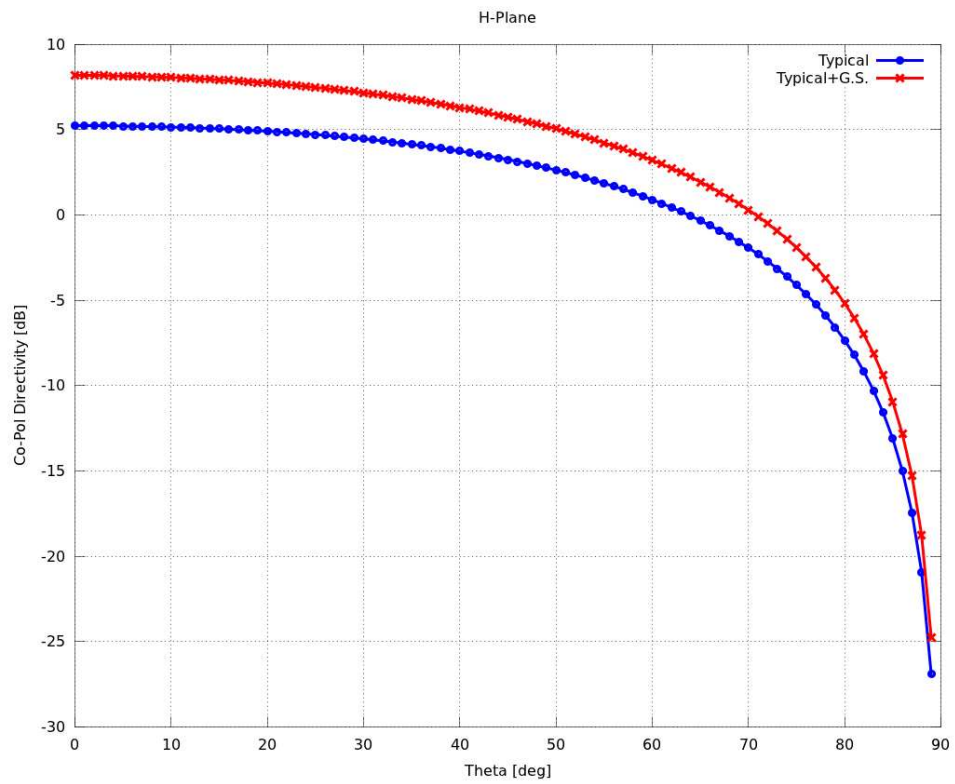
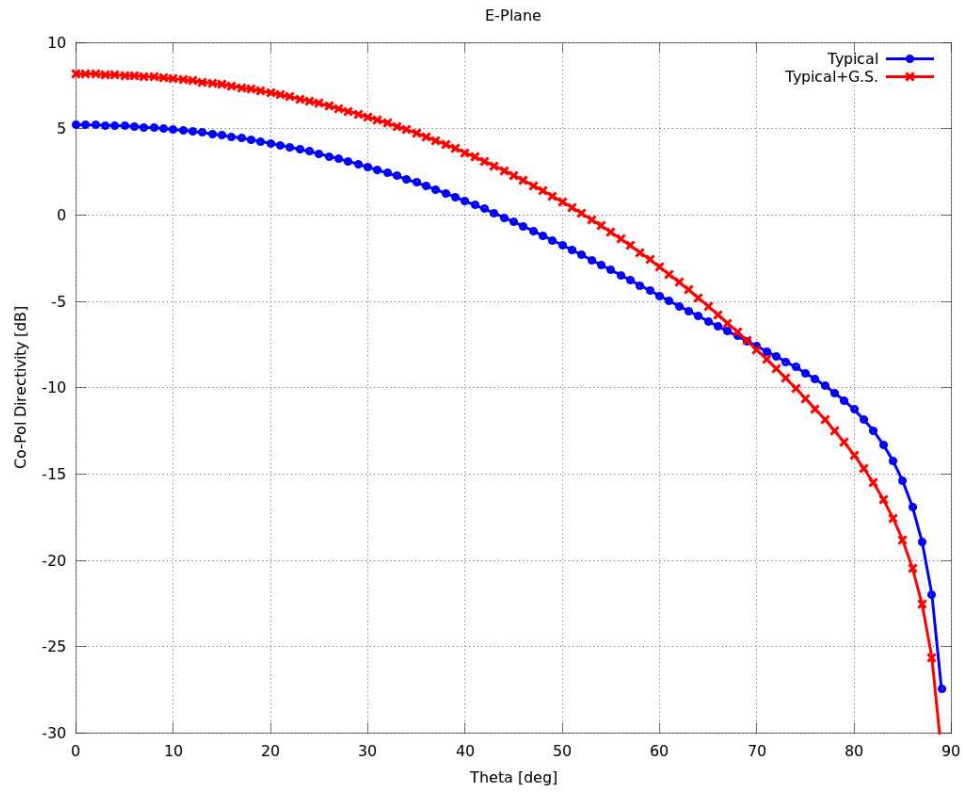


Figure 8: 30 MHz co-polarized directivity of the candidate LEDA antenna with and without ground screen. In both cases, “typical” ($\epsilon_r = 13$, $\sigma = 5$ mS/m) ground is assumed.

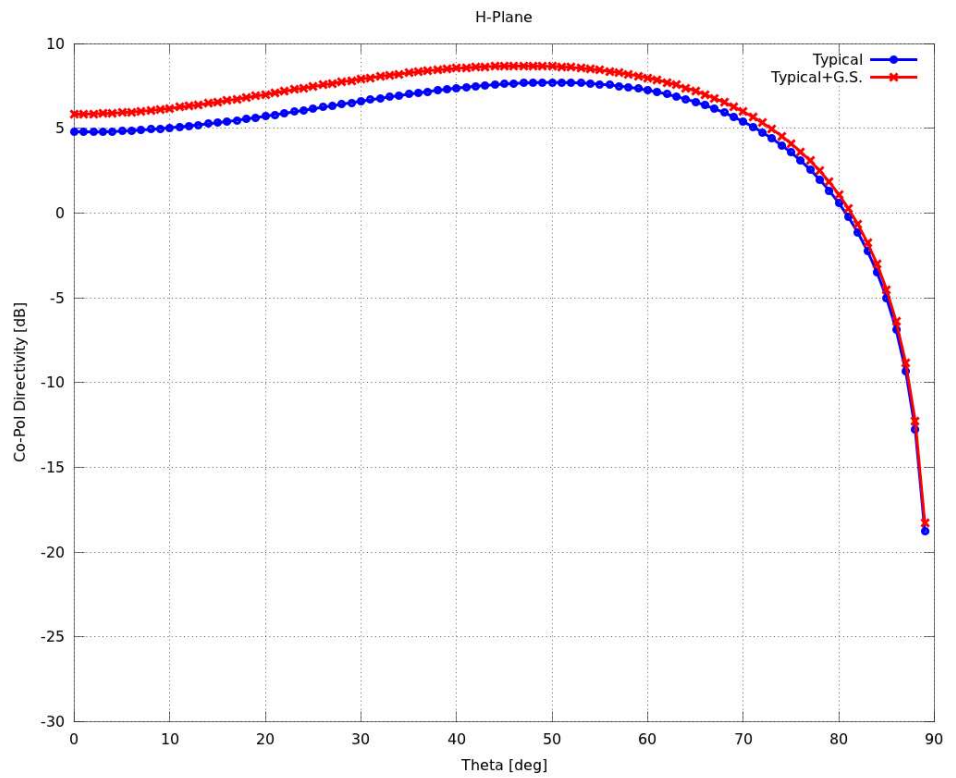
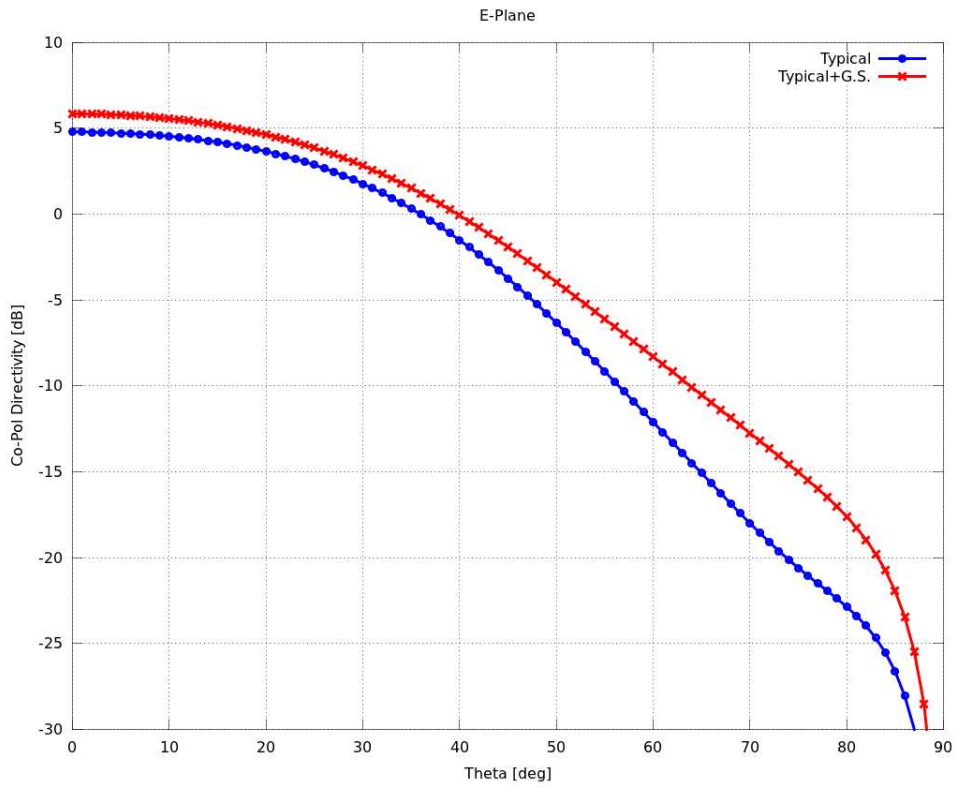


Figure 9: 88 MHz co-polarized directivity of the candidate LEDA antenna with and without ground screen. In both cases, “typical” ($\epsilon_r = 13$, $\sigma = 5$ mS/m) ground is assumed.

6 Acknowledgments

Thanks to A.E.E. Rogers of MIT/Haystack for providing unpublished technical details about four-point antennas developed for EDGES.

References

- [1] J. D. Bowman, A. E. E. Rogers, and J. N. Hewitt (2008), “Toward Empirical Constraints on the Global Redshifted 21 cm Brightness Temperature During the Epoch of Reionization,” *Astrophysical J.*, 676, 1.
- [2] S.Y. Suh, *A Comprehensive Investigation of New Planar Wideband Antennas*, Ph.D. Dissertation, Virginia Polytechnic Institute & State University, 2002.
- [3] A. E. E. Rogers and J. D. Bowman (2008), “Spectral Index of the Diffuse Radio Background Measured from 100 to 200 MHz,” *Astronomical J.*, 136, 641.
- [4] A. E. E. Rogers (2011), “Optimization of EDGES Fourpoint antenna using FEKO,” EDGES Memo 69, [online]
http://www.haystack.mit.edu/ast/arrays/Edges/EDGES_memos/EdgesMemo.html.
- [5] G. J. Burke, “Numerical Electromagnetics Code – NEC-4 Method of Moments,” Lawrence Livermore National Laboratory Tech. Rep. UCRL-MA-109338, Jan. 1992, Parts I-III.
- [6] S.W. Ellingson, “Sensitivity of Antenna Arrays for Long-Wavelength Radio Astronomy,” *IEEE Trans. Ant. & Prop.*, Vol. 59, No. 6, June 2011, pp. 1855-1863.
- [7] S.W. Ellingson, J.H. Simonetti, and C.D. Patterson, “Design and Evaluation of an Active Antenna for a 29–47 MHz Radio Telescope Array,” *IEEE Trans. Ant. & Prop.*, Vol. 55, No. 3, March 2007, pp. 826-831.